Attenuation of Vibrational Interference -Robust and Adaptive Approaches

Tudor-Bogdan Airimitoaie, Ioan Doré Landau

Attenuation of Vibrational Interference - Robust and Adaptive Approaches

Tudor-Bogdan Airimiţoaie[1] and Ioan Doré Landau[2]

***Abstract*— Vibration interference appears when the frequency of two vibrations are very close. This generates in addition a low frequency disturbance which absolutely need to be strongly attenuated since its impact can be very damaging on some applications. The paper considers the case of simultaneous vibration interference occurring in two different regions in the frequency domain. The frequency of the vibrations is varying but within a limited frequency range. A feedback approach is considered and two solutions are proposed. The first is a robust linear controller which has been designed taking advantage of the knowledge of the domains of variation of the frequencies of the vibrations. However the performance of the linear controller is somehow limited because of the width of the regions of variation of the frequencies of the vibrations and the robustness constraints. To further improve the performance, a direct adaptive regulation algorithm will be added. The methodology is illustrated by its implementation on a relevant test bench for active vibration control.**

I. Introduction

A pertinent problem encountered in the practice of Active Vibration Control (AVC) is the attenuation of the vibrational interference. Vibrational interference appear when the frequency of two vibrations are very close. This generates in addition a very low frequency disturbance which absolutely has to be strongly attenuated since its impact can be very damaging. A typical image of the phenomenon is shown in Fig. 1 and an example of mechanical system presenting this phenomenon is given in [1].

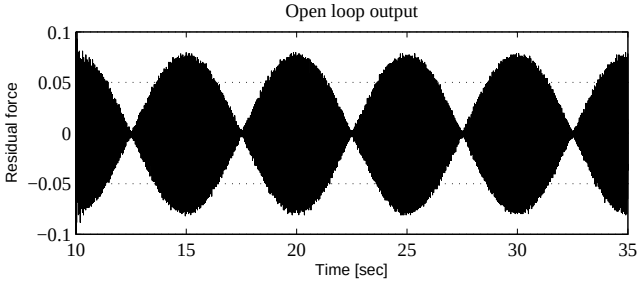

Fig. 1. Vibrational interference of two sinusoidal disturbances.

In this paper, one considers the case of simultaneous vibration interference occurring in two different regions in the frequency domain. The frequency of the vibrations is varying but within a limited frequency range.

Vibrations in terms of control terminology are "disturbances" which have to be compensated. In AVC, to attenuate vibrations two approaches are considered: (i) feedforward compensation and (ii) feedback compensation. The feedforward compensation has a number of disadvantages (see [2]); the most important are the need for an additional transducer and the presence of an internal positive feedback. While this approach has to be used when the disturbances are wide band, its use is not justified for the case of narrow or tonal disturbances. In this paper a feedback approach will be considered and only a measurement of the residual acceleration (or force) will be used.

In managing the vibration attenuation by feedback, the shape of the modulus of the "output sensitivity function" (the transfer function between the disturbance and the residual acceleration/force) is fundamental both from performance and robustness considerations. Three basic concepts are to be considered: the Bode Integral, the Modulus margin and the Internal Model Principle (IMP).

Several problems have been considered in the field of active vibration control by feedback only. The case of full rejection of single or multiple tonal disturbances (up to 3) located quite distantly in the frequency domain with unknown and time varying frequencies over a significant frequency range has been extensively covered in the literature. An adaptive feedback approach taking advantage of the IMP as well as of a special parametrization of the controller (the Youla-Kučera parametrization [3]) has been considered. An international benchmark has been organized where various techniques have been comparatively evaluated on an experimental test bench [4].[1]

Since in the problem considered in this paper the disturbances are located within two relatively small frequency ranges, it is possible to consider a linear control design which will shape the output sensitivity function in such a way that a sufficient attenuation is introduced in these two frequency regions but avoiding significant amplification at other frequencies (both for performance and robustness reason). This problem in the context of active noise control has been considered in [5] and the shaping of the output sensitivity function has been achieved using the convex optimization procedure introduced in [6]. A H_∞ approach can also eventually be used but it will require a quite

*This work was not supported by any organization.

[1]Tudor-Bogdan Airimiţoaie is with the Univ. Bordeaux, IMS, UMR 5218, F-33405 Talence, France. tudor-bogdan.airimitoaie@u-bordeaux.fr

[2]Ioan Doré Landau is with CNRS, GIPSA-lab, UMR 5216, F-38402 Saint Martin D'Hères, France. ioan-dore.landau@gipsa-lab.grenoble-inp.fr

[1]More details can be found on the website http://www.gipsa-lab.grenoble-inp.fr/~ioandore.landau/benchmark_adaptive_regulation/

complicated procedure for defining the appropriate weighting functions. It will be shown in this paper that an elementary procedure for shaping appropriately the modulus of the sensitivity functions can be implemented using stop band filters as shaping tools. For a basic reference on this approach see [7].

To further improve the performance, an algorithm for direct adaptive rejection of the disturbances will be added [8]. This algorithm takes into account the IMP and uses the Youla-Kučera (YK) parametrization of the controller. It has been introduced in [8] and has been used in different contexts including the benchmark mentioned above. It is however for the first time that it is used in the context of four simultaneous time varying and unknown sinusoidal disturbances which are very close each other two by two.

Another important point of the methodology for designing AVC systems is the fact that one uses for design discrete-time models of the system directly estimated from data (both the orders of the model and the parameters). The system is considered as a "black box."

II. System Presentation

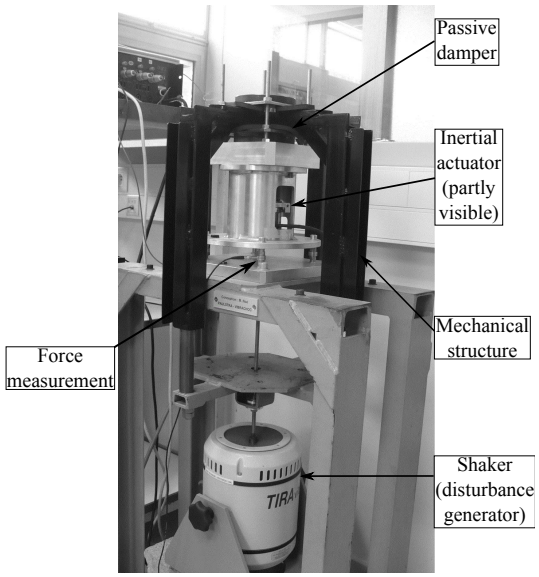

Fig. 2. The active vibration control system (photo).

The AVC system that will be used for the experiments is shown in Fig. 2. The same system has been used for an international benchmark on adaptive disturbance regulation (see [4]). It consists of a shaker (fixed to the ground), a passive damper, an inertial actuator, a mechanical structure, and a transducer for the residual force. For control purposes, 2 desktop computers are used, one with a Microsoft Windows operating system and Matlab/Simulink environment (for controller design, implementation and simulation) and the second with the real time operating system Matlab xPC Target (for real-time operation of the AVC system) - see also the benchmark website[1] for more information.

The mechanical construction is such that the vibrations produced by the shaker are transmitted to the upper part of the mechanical structure, on top of the passive damper. The inertial actuator is fixed to the chassis where the vibrations should be attenuated. The controller, through a power amplifier, generates current in the coil which produces motion in order to reduce the residual force. The control signal $u(t)$ represents the position of the magnet inside the inertial actuator. The measured output of the system (residual force) is $y(t)$ which enters the xPC Target dedicated computer for real time control and data acquisition. Finally, for testing purposes, the disturbance $p(t)$ induced by the shaker on the residual force is operated from the computer through the disturbance input $u_p(t)$. The transfer function between the disturbance input $u_p(t)$ and the measured output $y(t)$ is called *primary path*. The transfer function between the control input $u(t)$ and the measured output is called *secondary path*. Note that the system has a double differentiator behavior (input=position, output=force).

The control objective is to attenuate the effect of unknown time-varying narrow-band disturbances on the residual force measurement. The physical parameters of the system being unknown, black-box discrete time linear model identification has to be done in order to obtain a dynamical model of the primary and secondary paths.[2] The sampling period is $T_s = 0.00125$ sec ($f_s = 800$ Hz).

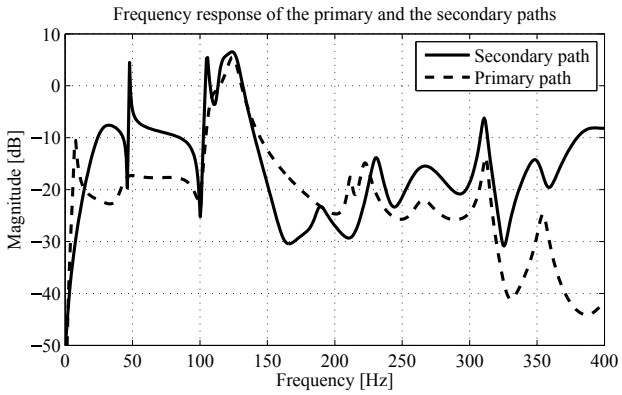

Fig. 3. Frequency characteristics of the secondary and the primary paths.

Fig. 3 gives the frequency characteristics of the identified model for the primary and secondary paths. As it can be seen, there is an important number of very low damped complex poles (resonances) and complex zeros (anti-resonances). The primary path model is used only for simulation purposes.

III. System Description

The linear time invariant (LTI) discrete time model of the secondary path, used for controller design is

$$G(z^{-1}) = \frac{z^{-d}B(z^{-1})}{A(z^{-1})} = \frac{z^{-d-1}B^*(z^{-1})}{A(z^{-1})}, \qquad (1)$$

where

$$A(z^{-1}) = 1 + a_1 z^{-1} + \cdots + a_{n_A} z^{-n_A}, \qquad (2)$$

$$B(z^{-1}) = b_1 z^{-1} + \cdots + b_{n_B} z^{-n_B} = z^{-1} B^*(z^{-1}), \qquad (3)$$

[2]Both the orders and the parameters of the models have been estimated from data.

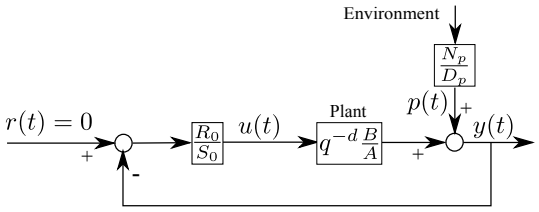

Fig. 4. Feedback regulation scheme for rejection of disturbances.

and d is the plant pure time delay in number of sampling periods.[3]

The output of the plant $y(t)$ and the input $u(t)$ may be written as (see Fig. 4):

$$y(t) = \frac{q^{-d}B(q^{-1})}{A(q^{-1})} \cdot u(t) + p(t), \tag{4}$$

$$S_0(q^{-1}) \cdot u(t) = -R_0(q^{-1}) \cdot y(t). \tag{5}$$

In (4), $p(t)$ is the effect of the disturbances on the measured output[4] and $R_0(z^{-1})$, $S_0(z^{-1})$ are polynomials in z^{-1} having the following expressions[5]:

$$S_0 = 1 + s_1^0 z^{-1} + \ldots + s_{n_S}^0 z^{-n_S} = S_0' \cdot H_{S_0}, \tag{6}$$

$$R_0 = r_0^0 + r_1^0 z^{-1} + \ldots + r_{n_R}^0 z^{-n_R} = R_0' \cdot H_{R_0}, \tag{7}$$

where $H_{S_0}(z^{-1})$ and $H_{R_0}(z^{-1})$ represent pre-specified parts of the controller (used for example to incorporate the internal model of a disturbance or to open the loop at certain frequencies) and $S_0'(z^{-1})$ and $R_0'(z^{-1})$ are the solutions of the Bezout equation

$$P_0 = (A \cdot H_{S_0}) \cdot S_0' + \left(z^{-d}B \cdot H_{R_0}\right) \cdot R_0'. \tag{8}$$

In the last equation, $P_0(z^{-1})$ represents the characteristic polynomial, which specifies the desired closed loop poles of the system.

The transfer functions between the disturbance $p(t)$ and the output of the system $y(t)$ and from disturbance to the control input $u(t)$, denoted respectively *output sensitivity function* and *input sensitivity function*, are given by

$$S_{yp}(z^{-1}) = \frac{A(z^{-1})S_0(z^{-1})}{P_0(z^{-1})} \tag{9}$$

and

$$S_{up}(z^{-1}) = -\frac{A(z^{-1})R_0(z^{-1})}{P_0(z^{-1})}. \tag{10}$$

It is important to remark that one should only reject disturbances located in frequency regions where the plant model has enough gain. This rule results from (9) and noticing that perfect rejection at a certain frequency ω_0 is obtained *iff* $S_0(e^{-j\omega_0}) = 0$. At this frequency, under perfect rejection of disturbances, one gets

$$S_{up}(e^{-j\omega_0}) = -\frac{AR_0}{0 + e^{-dj\omega_0}BR_0} = -\frac{A}{e^{-dj\omega_0}B} = \frac{1}{G(e^{-j\omega_0})}. \tag{11}$$

Equation (11) corresponds to the inverse of the gain of the system to be controlled. Its implication is that cancellation (or in general an important attenuation) of disturbances on the output should be done only in frequency regions where the system gain is large enough. If the gain of the controlled system is too low, $|S_{up}|$ will be large at these frequencies. Therefore, the robustness vs additive plant model uncertainties will be reduced and the stress on the actuator will become important [7]. Equation (11) also implies that serious problems will occur if $B(z^{-1})$ has complex zeros close to the unit circle (stable or unstable zeros) at frequencies where an important attenuation of disturbances is required. It is mandatory to avoid attenuation of disturbances at these frequencies.

IV. Robust Control Design

In this section, the design of a linear robust digital controller for disturbance attenuation is presented. Before presenting the objectives for regulation and robustness, a few notions about feedback disturbance attenuation should be reminded. In the case of a feedback controlled system, the Bode integral constraint leads to a waterbed effect on the output sensitivity function (defined in Section III). In other words, forcing the magnitude of the output sensitivity function at certain frequencies below 0 dB (in order to attenuate disturbances) has an inverse effect at neighboring frequencies, where an amplification will be observed. Recalling from [7] that the minimal distance between the Nyquist plot of the open loop transfer function and the critical point $-1 + 0i$ (also called *modulus margin*) corresponds to the inverse of the maximum of the output sensitivity function, it can be concluded that "too much" attenuation at some frequencies can have a bad effect on the robust stability of the closed loop system.

Taking into consideration the secondary path frequency response in Fig. 3 and the fact that disturbances can only be attenuated where the system has enough gain (see Section III) it has been concluded that only disturbances within the 50 Hz - 95 Hz frequency band can be attenuated.

For the design of the linear robust digital controller the following specifications are considered: (i) up to 4 sines disturbances are supposed to affect the output of the system (known structure of the disturbance model), (ii) their frequencies are not known exactly but they are varying within a ± 2.5 Hz frequency band around 60 Hz and 80 Hz, (iii) the controller should attenuate the disturbances by a minimum of 14 dB, (iv) the maximum allowed amplification of the output sensitivity function is of 8 dB, (v) the effect of disturbances on the control input should be attenuated above 100 Hz in order to improve robustness with respect to unmodeled dynamics and nonlinear phenomena ($S_{up}(e^{-j\omega}) < -20$ dB, $\forall \omega \in [100\text{ Hz}, 400\text{ Hz}]$), (vi) the

[3]The complex variable z^{-1} will be used to characterize the system's behavior in the frequency domain and the delay operator q^{-1} will be used for the time domain analysis.

[4]The disturbance passes through a so called *primary path* and $p(t)$ is its output.

[5]The argument (z^{-1}) will be omitted in some of the following equations to make them more compact.

gain of the controller has to be zero at zero frequencies (since the system has a double differentiator behavior), and (vii) the gain of the controller should be zero at $0.5f_s$ where the system has low gain and uncertainties exist.

It is shown in [7, Property 7, Section 3.6.1] that very accurate shaping of the output or the input sensitivity function can be obtained by the use of band-stop filters (BSF). These are IIR filters obtained from the discretization of continuous-time filters of the form $F(s) = \frac{s^2+2\zeta_{num}\omega_0 s+\omega_0^2}{s^2+2\zeta_{den}\omega_0 s+\omega_0^2}$ using the bilinear transform $s = \frac{2}{Ts}\frac{1-z^{-1}}{1+z^{-1}}$. The use of BSFs introduces an attenuation $M = 20\log\left(\frac{\zeta_{num}}{\zeta_{den}}\right)$ at the normalized discretized frequency $\omega_d = 2\cdot\arctan\left(\frac{\omega_0 T_S}{2}\right)$. Depending on whether the filter is designed for shaping the output or the input sensitivity function, the numerator of the discretized filter is included in the fixed part of the controller denominator H_{S_0} or numerator H_{R_0}, respectively. The filter denominator is always included in the closed loop characteristic polynomial. As such, the filter denominator influences the design of the controller indirectly in the computation of S_0' and R_0' as solutions of the Bezout equation (8). They will be used for a fine shaping of both the output and input sensitivity functions.

The steps for the design of the linear controller are:[6] (i) include all (stable) secondary path poles in the closed loop characteristic polynomial for getting a good robustness, (ii) open the loop at 0 Hz and at 400 Hz by setting the fixed part of the controller numerator $H_R = (1+q^{-1})\cdot(1-q^{-1})$, (iii) 3 BSFs on S_{yp} have been used around each of the frequencies where attenuation is desired in order to assure the desired attenuation within ± 2.5 Hz (see Table I for specifications), (iv) 1 BSF has been used on S_{up} to reduce its magnitude above 100 Hz (see Table I for specifications), and (v) to improve robustness 2 complex conjugate poles have been added to the characteristic polynomial, one at 55 Hz and the second at 95 Hz, both of them with 0.1 damping factor.

TABLE I

BAND-STOP FILTERS FOR OUTPUT AND INPUT SENSITIVITY FUNCTIONS.

	Frequency [Hz]	**Amplification [dB]**	**Damping**
S_{yp}	57.5	-17	0.1
	59.8	-25	0.5
	62	-15	0.1
	77.5	-13	0.05
	79.8	-20	0.2
	82	-12	0.05
S_{up}	155	-16	0.5

The output and input sensitivity functions with this linear controller can be analyzed in Figs. 5 and 6 respectively. From Fig. 5, it can be observed that the desired attenuation and the maximum amplification of 8 dB on S_{yp} are achieved. The specification of -20 dB attenuation on S_{up} above 100 Hz are satisfied.

[6]The software iREG has been used for the design of this robust digital controller but the same results can be obtained using functions written in Matlab/Scilab languages (see `http://www.gipsa-lab.grenoble-inp.fr/~ioandore.landau/identificationandcontrol/`).

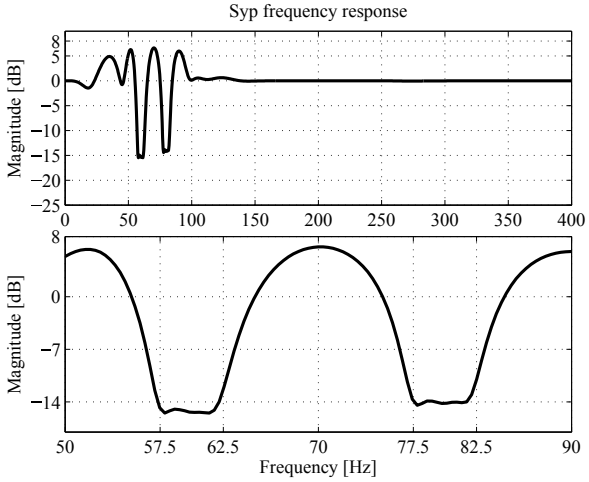

Fig. 5. Output sensitivity function with the linear controller (upper figure) and zoom in the 50 Hz to 90 Hz frequency interval (lower figure).

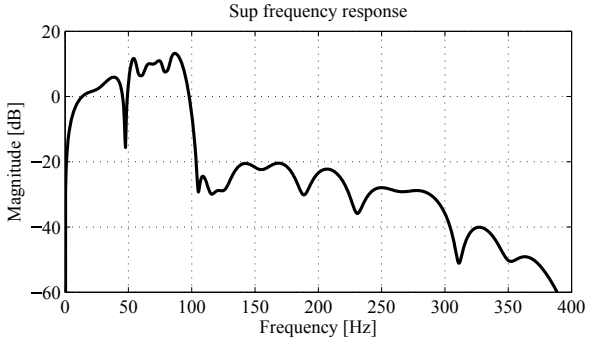

Fig. 6. Input sensitivity function with the linear controller.

V. ADAPTIVE FEEDBACK CONTROL

This section gives a brief presentation of the direct adaptive control scheme implemented on top of the central controller. The Youla-Kučera (YK) parametrization of the controller is used (see [3]) for implementing the adaptive loop. In this context, the controller polynomials are parametrized using an finite impulse response (FIR) filter of the form

$$Q(z^{-1}) = q_0 + q_1 z^{-1} + \ldots + q_{n_Q} z^{-n_Q}, \qquad (12)$$

and the central controller polynomials given in (6) and (7) obtained as solutions of the Bezout equation (8). As such, the controller polynomials become[7]

$$R = R_0 + AQH_{S_0}H_{R_0}, \qquad (13)$$

$$S = S_0 - z^{-d}BQH_{S_0}H_{R_0}. \qquad (14)$$

The purpose of the central controller ($\frac{R_0}{S_0}$) in the Youla-Kučera parametrization is that of verifying stability and robustness specifications. It should be observed that the characteristic polynomial of the closed loop remains unchanged

$$P = AS + z^{-d}BR = AS_0 + z^{-d}BR_0, \qquad (15)$$

[7]It is supposed that a very good model of the system is available so that $\hat{A} = A$ and $\hat{B} = B$.

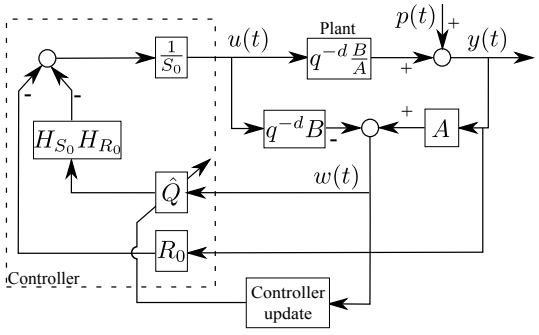

Fig. 7. Direct adaptive regulation scheme for rejection of unknown disturbances using the Youla-Kučera parametrization.

as such, the stability of the closed loop will not be influenced by the $Q(z^{-1})$ FIR filter. The role of the Q filter, which will be adjusted in real time using a parameter adaptation algorithm, is to assure the rejection of unknown time-varying disturbances using the IMP. The schematic representation of the closed loop with the adaptive Youla-Kučera parametrized controller of (13) and (14) is shown in Fig. 7.

A key aspect of this methodology is the use of IMP. It is supposed that $p(t)$ is a deterministic disturbance given by

$$p(t) = \frac{N_p(q^{-1})}{D_p(q^{-1})} \cdot \delta(t), \tag{16}$$

where $\delta(t)$ is a Dirac impulse and N_p, D_p are coprime polynomials of degrees n_{N_p} and n_{D_p}, respectively.[8] In the case of stationary narrow-band disturbances, the roots of $D_p(z^{-1})$ are on the unit circle. The noise/disturbance ratio is very low so the noise will not influence the convergence of the algorithm (it also can be shown, with the analysis tools given in [9], that the measurement noise will not influence the convergence of the algorithm for the case of decreasing adaptation gain algorithm).

Internal Model Principle: The effect of the disturbance (16) upon the output

$$y(t) = \frac{A(q^{-1})S(q^{-1})}{P(q^{-1})} \cdot \frac{N_p(q^{-1})}{D_p(q^{-1})} \cdot \delta(t), \tag{17}$$

where $D_p(z^{-1})$ is a polynomial with roots on the unit circle and $P(z^{-1})$ is an asymptotically stable polynomial, converges asymptotically towards zero *iff* the polynomial $S(z^{-1})$ in the RS controller has the form (based on eq. (6))

$$S(z^{-1}) = D_p(z^{-1})H_{S_0}(z^{-1})S'(z^{-1}). \tag{18}$$

Thus, the pre-specified part of $S(z^{-1})$ should be chosen as $H_S(z^{-1}) = D_p(z^{-1})H_{S_0}(z^{-1})$ and the controller is computed solving

$$P = AD_pH_{S_0}S' + z^{-d}BH_{R_0}R', \tag{19}$$

where P, D_p, A, B, H_{R_0}, H_{S_0} and d are given.[9] The Q polynomial allows the introduction in the controller of the model of the disturbance (i.e. if D_p is the model of the disturbance, it exist a polynomial Q of order $n_{D_p} - 1$ such that S given by (14) can be factorized as $S'D_p$ - see [9]).

Assuming that the structure of the disturbance is known, i.e. n_{D_p}, the order of the Q polynomial is fixed as $n_Q = n_{D_p} - 1$. Let define the estimate of Q at time t by $\hat{Q}(t, q^{-1}) = \hat{q}_0(t) + \hat{q}_1(t)q^{-1} + \ldots + \hat{q}_{n_Q}(t)q^{-n_Q}$ and the associated estimated parameter vector $\hat{\theta}(t) = [\hat{q}_0(t)\ \hat{q}_1(t)\ \ldots\ \hat{q}_{n_Q}(t)]^T$. Define the fixed parameter vector corresponding to the optimal value of the polynomial Q as: $\theta = [q_0\ q_1\ \ldots\ q_{n_Q}]^T$. Denote

$$w(t+1) = A \cdot y(t+1) - q^{-d}B^* \cdot u(t), \tag{20}$$

$$w_1(t) = \frac{S_0}{P} \cdot w(t),\ w_2(t) = \frac{q^{-d}B^*H_{S_0}H_{R_0}}{P} \cdot w(t) \tag{21}$$

and define the following observation vector

$$\phi^T(t) = [w_2(t)\ w_2(t-1)\ \ldots\ w_2(t-n_Q)]. \tag{22}$$

The *a priori* adaptation error can be defined as (see [8] for more details)

$$\varepsilon^0(t+1) = w_1(t+1) - \hat{\theta}^T(t)\phi(t). \tag{23}$$

For the estimation of the parameters of $\hat{Q}(t, q^{-1})$ an "Integral" Parameter Adaptation Algorithm (I-PAA) is used:

$$\hat{\theta}(t+1) = \hat{\theta}(t) + F(t)\phi(t)\varepsilon(t+1), \tag{24a}$$

$$\varepsilon(t+1) = \frac{\varepsilon^0(t+1)}{1 + \phi^T(t)F(t)\phi(t)}, \tag{24b}$$

$$\varepsilon^0(t+1) = w_1(t+1) - \hat{\theta}^T(t)\phi(t), \tag{24c}$$

$$F(t+1) = \frac{1}{\lambda_1(t)}\left[F(t) - \frac{F(t)\phi(t)\phi^T(t)F(t)}{\frac{\lambda_1(t)}{\lambda_2(t)} + \phi^T(t)F(t)\phi(t)}\right],$$
$$1 \geq \lambda_1(t) > 0,\ 0 \leq \lambda_2(t) < 2, \tag{24d}$$

where $\lambda_1(t)$, $\lambda_2(t)$ allow to obtain various profiles for the evolution of the adaption gain $F(t)$ (for more details see [9]). Stability analysis for this algorithm has been done in [8]. Another more general choice of adaptation algorithm is the "Integral+Proportional" Parameter Adaptation Algorithm (IP-PAA) (see [9], [10] for more details).

VI. Experimental Results

The experimental results presented in this section are obtained using the identified model of the secondary path (see also Section II). Details on system identification and the model used throughout this section can be found on the benchmark web.[10] The secondary path model is given in the file *model_sec2.mat*. The orders of this system are: $n_A = 22$, $n_B = 25$, and $d = 0$.

[8]Throughout the paper, n_X denotes the degree of the polynomial X.

[9]Of course, it is assumed that D_p and B do not have common factors.

[10]http://www.gipsa-lab.grenoble-inp.fr/~ioandore.landau/benchmark_adaptive_regulation/files/Simulator_2.zip

A. Central Controller for Youla-Kučera Parametrization

The design of the central controller used in the Youla-Kučera parametrization is similar to the design of the robust linear controller with the exception that the BSFs on S_{yp} have not been used and the resulting free roots to be assigned have been moved from 0 to 0.2. Remark that the order of the characteristic polynomial is given by $n_P = n_A + n_B + n_{H_S} + n_{H_R} + d - 1$ which in our case gives $22+25+0+4+0-1 = 50$. Given the roots already specified (28 as can be concluded from the design of the robust controller excepting roots given by BSFs for S_{yp}), it follows that 22 roots can be selected. These 22 auxiliary poles at 0.2 have the effect of reducing the magnitude of S_{up} above 100 Hz. They were not used in the robust linear design.

B. Vibrational Interference Control (Two-Mode Vibration Control)

This subsection deals with the AVC of vibrational interference of sinusoidal disturbances. It can be shown (see also [11]) that when two sinusoidal disturbances are close enough, a vibrational interference phenomena appears due to the periodic cancellation of the two neighboring sinusoidal disturbances. This phenomena is shown in Fig. 1 where 2 pairs of neighboring sinusoidal disturbances are introduced, one pair around 60 Hz (at 59.9 and 60.1 Hz) and the second around 80 Hz (at 79.9 and 80.1 Hz).

Note that all subsequent experiments start at 10 seconds (time needed to activate the electronic boards for real time experimentation). Also, the system operates in open loop for 5 seconds (from 10 to 15 sec). Finally, 5 seconds before the end of the experiments, the system is switched back to open loop and the system input and the disturbances are removed.

To avoid large transients when switching on the controllers, a bumpless transfer scheme from open to closed loop has been used (see also [7, Chapter 8]).

The robust linear controller designed in Section IV will be used. For adaptive regulation, the I-PAA has been used with an initial diagonal adaptation gain matrix $F(0) = \alpha \cdot I$, with $\alpha = 0.2$ and I the identity matrix (initial trace of 0.8), and a decreasing gain followed by constant trace adaptation. The constant trace is chosen equal to 0.02. The number of parameters for the Q polynomial is also equal to 4 (order equal to 3). Augmenting the order of the polynomial Q to 7 (8 parameters - two for each sinusoidal disturbance) does not improve the performance (probably because the frequencies of the pair of sines are too close).

Time domain results are shown in Fig. 8. The global attenuation for the robust linear controller is 27.50 dB and for the adaptive controller is 45.59 dB. Power spectral densities (PSD) estimates of the two control schemes are given in Fig. 9. The attenuation introduced by the robust linear controller in the desired frequency zone is equal to 14 dB which is coherent with the design done in Section IV. The adaptive regulator has better attenuation of disturbances and also does not amplify at other frequencies more than the linear controller.

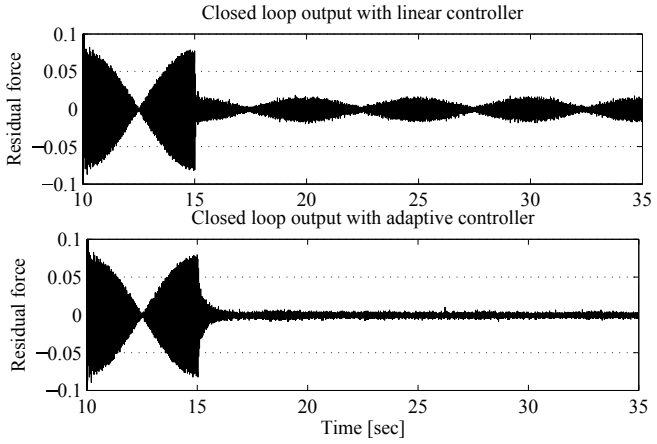

Fig. 8. Residual force in closed loop with linear controller (upper plot) and with adaptive controller (lower plot). The loop is closed at t=15 sec.

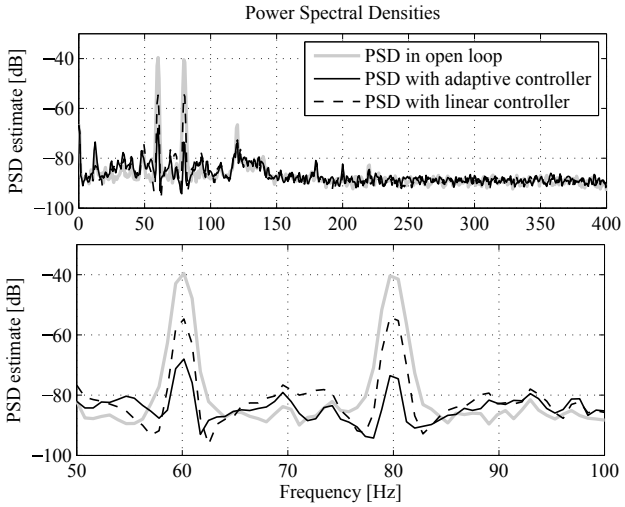

Fig. 9. Power spectral densities of the open loop, robust linear controller, and adaptive regulator. Full frequency range in the upper plot, zoom between 50 and 100 Hz in the lower plot.

Adaptation capabilities are tested for a step frequency change of 5 Hz for all 4 sinusoids and results are shown in Fig. 10. The change occurs at 35 seconds. The adaptation transient is about 1.5 sec.

VII. Conclusion

It was shown in this paper that strong attenuation of the vibrational interference can be achieved. Since the range of frequency variation is limited, an efficient robust active compensation can be achieved with a properly designed linear controller. However, adding an adaptive loop enhances drastically the performance. The use of the adaptive approach allows to expand the range of frequency variations of the vibrations for which the desired level of performance is achieved. In this new context the performance of the robust controller are unsatisfactory.

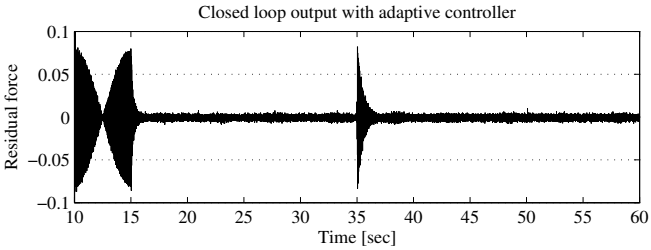

Fig. 10. Residual force with step frequency changes (+5 Hz) in closed loop with adaptive controller. The system is in open loop until t=15 sec.

REFERENCES

[1] X. Zhang, X. Li, H. Hao, D. Wang, and Y. Li, "A case study of interior low-frequency noise from box-shaped bridge girders induced by running trains: Its mechanism, prediction and countermeasures," *Journal of Sound and Vibration*, vol. 367, pp. 129 – 144, 2016.

[2] I. D. Landau, T.-B. Airimiţoaie, and A. Castellanos Silva, "Adaptive attenuation of unknown and time-varying narrow band and broadband disturbances," *International Journal of Adaptive Control and Signal Processing*, vol. 29, no. 11, pp. 1367–1390, 2015.

[3] B. Anderson, "From Youla-Kucera to identification, adaptive and nonlinear control," *Automatica*, vol. 34, pp. 1485–1506, 1998.

[4] I. D. Landau, A. Castellanos Silva, T.-B. Airimiţoaie, G. Buche, and M. Noé, "Benchmark on adaptive regulation: rejection of unknown/time-varying multiple narrow band disturbances," *European Journal of Control*, vol. 19, no. 4, pp. 237 – 252, 2013.

[5] J. C. Carmona and V. M. Alvarado, "Active noise control of a duct using robust control theory," *IEEE Transactions on Control Systems Technology*, vol. 8, no. 6, pp. 930–938, 2000.

[6] J. Langer and I. D. Landau, "Combined pole placement/sensitivity function shaping method using convex optimization criteria," *Automatica*, vol. 35, no. 6, pp. 1111–1120, 1999.

[7] I. D. Landau and G. Zito, *Digital Control Systems - Design, Identification and Implementation*. London: Springer, 2005.

[8] I. D. Landau, A. Constantinescu, and D. Rey, "Adaptive narrow band disturbance rejection applied to an active suspension - an internal model principle approach," *Automatica*, vol. 41, no. 4, pp. 563–574, 2005.

[9] I. D. Landau, R. Lozano, M. M'Saad, and A. Karimi, *Adaptive control*, 2nd ed. London: Springer, 2011.

[10] T.-B. Airimiţoaie and I. D. Landau, "Improving adaptive feedforward vibration compensation by using "Integral+Proportional" adaptation," *Automatica*, vol. 49, no. 5, pp. 1501 – 1505, 2013.

[11] S. Li, J. Li, and Y. Mo, "Piezoelectric Multimode Vibration Control for Stiffened Plate Using ADRC-Based Acceleration Compensation," *IEEE Transactions on Industrial Electronics*, vol. 61, no. 12, pp. 6892–6902, 2014.